Applied Surface Science 330 (2015) 216–220

Contents lists available at ScienceDirect

Applied Surface Science

journal homepage: www.elsevier.com/locate/apsusc

Fabrication and hyperthermia effect of magnetic functional fluids based on amorphous particles

Chuncheng Yang, Xiufang Bian*, Jingyu Qin, Tongxiao Guo, Shuchun Zhao

Key Laboratory for Liquid–Solid Structural Evolution and Processing of Materials, Ministry of Education, Shandong University, Jinan 250061, China

ARTICLE INFO

Article history:
Received 19 September 2014
Received in revised form
22 December 2014
Accepted 4 January 2015
Available online 12 January 2015

Keywords:
Magnetic functional fluids
Nanoparticles
Amorphous particles
Hyperthermia effect

ABSTRACT

An experimental study conducted on the preparation and hyperthermia effect of magnetic functional fluids based on $Fe_{73.5}Nb_3Cu_1Si_{13.5}B_9$ amorphous particles, $CoFe_2O_4$ nanoparticles and Fe_3O_4 nanoparticles dispersed in water is presented. Scanning electron microscopy, X-ray diffraction, differential scanning calorimetry and vibrating sample magnetometer methods have been used to characterize the morphology, structure and magnetic property of the amorphous particles. It is disclosed that the $Fe_{73.5}Nb_3Cu_1Si_{13.5}B_9$ particles are still amorphous after being milled for 48 h. Moreover, the saturation magnetization of metallic glass particles is approximately 75% and 50% larger than that of $CoFe_2O_4$ nanoparticles and Fe_3O_4 nanoparticles, respectively. The hyperthermia experiment results show that when alternating electrical current is 150 A, the temperature of the functional fluids based on amorphous particles could rise to 33 °C in 1500 s. When the current is 300 A, the final stable temperature could reach to 60 °C. This study demonstrates that the $Fe_{73.5}Nb_3Cu_1Si_{13.5}B_9$ magnetic functional fluids may have potential on biomedical applications.

1. Introduction

Magnetic functional fluids, a class of smart materials, have drawn considerable attention in both academia and industry as their rheological, electrical and thermal properties can be controlled under an applied external magnetic field [1–4]. Common magnetic functional fluids include magneto-rheological (MR) fluids and ferrofluids (FFs) [5–8]. MR fluids are suspensions micrometer-sized dispersed in liquid carrier [9]. Particles of this size (between 1 and 10 μm) are magnetically multidomain, which constitutes the physical reason for the distinctive characteristics of MR fluids. MR fluids can exhibit a rapid response when a magnetic field is applied, which makes suitable as shock absorbers and dampers in applications ranging from prosthetic legs to helicopters [10,11]. FFs (also called magnetic fluids or magnetic nanofluids) primarily consist of nano-size particles suspended in a carrier liquid, which exhibit simultaneously liquid and superparamagnetic properties [12]. FFs have been used in medical science for oncotherapy [13], chemical science for solid phase extraction [14] and machine science for senor [15], etc.

The magnetic particles used in MR fluids or FFs are usually magnetite (Fe_3O_4) or cobalt ferrite ($CoFe_2O_4$) because of their intriguing properties such as superparamagnetism and biocompatibility. However, the weak magnetic properties constrain their practical use in some areas such as high temperature cooling and elevated-temperature seals applications. The Fe-based amorphous alloys have broad prospects for industry applications due to their uniquely high magnetic properties relating to the short-range ordered and long-range disordered atomic structures as well as low cost of raw materials [16]. Nowadays, Fe-based amorphous alloys are becoming more widespread for efficient transformer cores application, as they are the most magnetically soft commercially available materials. Moreover, addition of amorphous alloy powders into FFs can give rise to a dramatic enhancement in decreasing chemical oxygen demand (COD) and decolorization [17]. Fe-based amorphous alloy particles have an excellent development potential in the application of magnetic functional fluids. However, detailed research of Fe-based amorphous alloy particle and its soft magnetic properties applied to functional fluids have not been yet significantly reported.

Hyperthermia is an extensively studied technique for cancer treatment [18]. Cancer treatment by hyperthermia consists in increasing artificially the temperature in the tumor up to 42–45 °C, which results in the death of carcinogenic cells.

* Corresponding author. Tel.: +86 531 88392748; fax: +86 531 88395011.
E-mail address: xfbian@sdu.edu.cn (X. Bian).

http://dx.doi.org/10.1016/j.apsusc.2015.01.023
0169-4332/

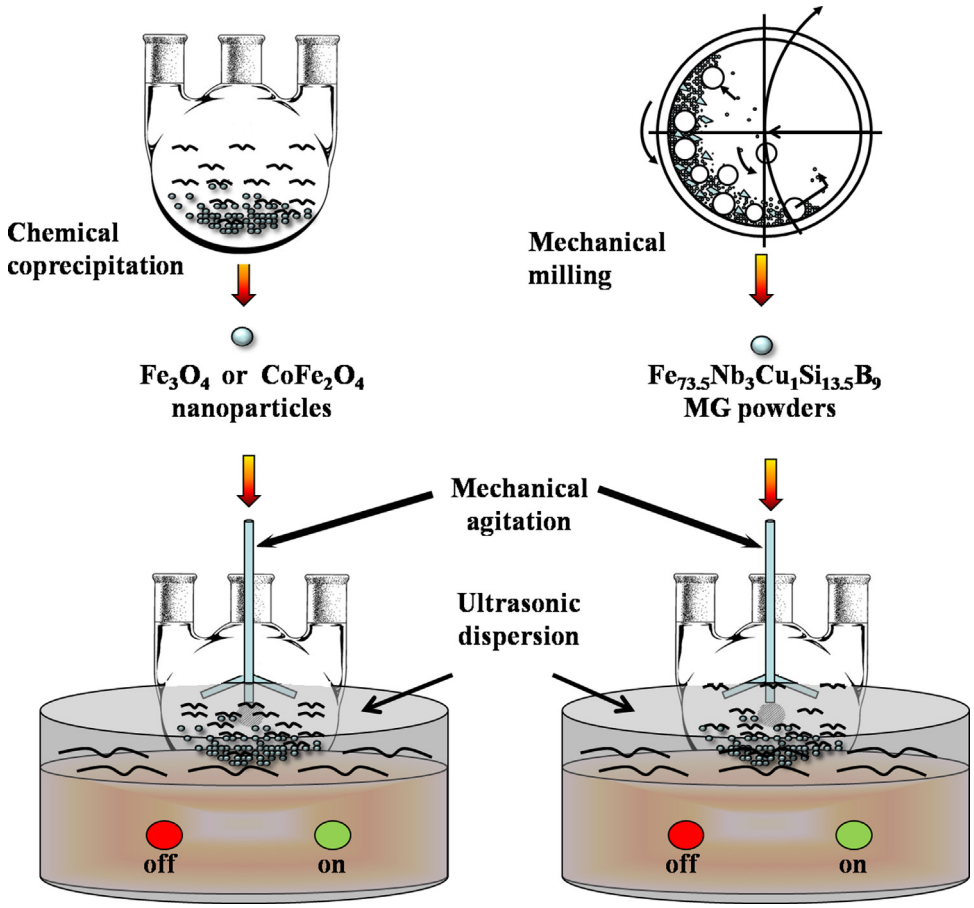

Fig. 1. The sketch of preparation of $Fe_{73.5}Nb_3Cu_1Si_{13.5}B_9$ MR fluid, Fe_3O_4 FF and $CoFe_2O_4$ FF.

Previously, microwave, laser and ultrasound radiation were used for hyperthermia. Nowadays, one of the most promising directions for hyperthermia is to use magnetic functional fluids as there is no undue heating of healthy tissues. When exposed to a low-frequency alternating magnetic field, the particles in fluids generate heat that destroys the tumor. Nevertheless, no reports have been done on hyperthermia research of magnetic functional fluids based on Fe-based amorphous particles.

Three kinds of magnetic functional fluids, $Fe_{73.5}Nb_3Cu_1Si_{13.5}B_9$ MR fluid, Fe_3O_4 FF and $CoFe_2O_4$ FF were prepared. The hyperthermia effect of these magnetic functional fluids was also investigated in this paper. Considering the excellent magnetic properties and obvious heating effect, the magnetic functional fluids based on Fe-based amorphous particles could offer opportunities in medical applications and other emerging applications such as magneto-caloric energy conversion devices [19], seals fields [20], cooling applications [21], as well as printed electronics [22], etc.

2. Experimental

All the chemicals used in the experiments were of analytical reagent (AR) grade without further purification. Before each experiment, all glassware were cleaned with dilute nitric and repeatedly washed with deionized water.

The Fe_3O_4 FF and $CoFe_2O_4$ FF used here were chemically synthesized through chemical co-precipitation method. A mixture solution of $FeCl_2{\cdot}4H_2O$ and $FeCl_3{\cdot}6H_2O$ with a molar ratio of 2:1 was dissolved in a three-necked flask. Then a certain amount of ammonia aqueous solution (25%) was added rapidly to it with mechanical stirring and supersonic dispersion. The black Fe_3O_4 nanoparticles were obtained by

$$2Fe^{3+} + Fe^{2+} + 8NH_3{\cdot}H_2O = Fe_3O_4 + 8NH_4{}^{+} + 4H_2O$$

A mixture solution of $FeCl_3{\cdot}6H_2O$ and $Co(NO_3)_2$ with a molar ratio of 2:1 was dissolved in a three-necked flask. Then a certain amount of NaOH solution was added rapidly and heated to boiling for 60 min with stirring. Then the mixture solution was cooled to room temperature. A black precipitate was obtained by

$$2Fe^{3+} + Co^{2+} + 8OH^{-} = CoFe_2O_4 + 4H_2O$$

After this, appropriate agar (0.075 g) and polyethylene glycol (0.05 g PEG-4000) were put into the Fe_3O_4 or $CoFe_2O_4$ suspension at a constant temperature as the first and second surfactant respectively. The mixture suspension was stirred at a constant temperature for 1 h. Finally, after being cooled to room temperature, the stable Fe_3O_4 and $CoFe_2O_4$ aqueous FFs were obtained.

As for the amorphous ribbons, ingots of $Fe_{73.5}Nb_3Cu_1Si_{13.5}B_9$ were prepared from the pure elements in an argon atmosphere. The prealloyed ingots were remelted by high-frequency induction heating and rapidly solidified into continuous ribbons at different circumferential speed in a controlled argon atmosphere. Ribbons were produced by a single roller melt-spinning device using a quartz crucible and a copper wheel of 350 mm in diameter under an argon atmosphere. The thickness of amorphous ribbons depends on the velocity of the wheel. Then the ribbons were milled 48 h with the rotating speed of 350 r/min under the high purity Ar gas for protection. Then the amorphous particles after being milled for 48 h were washed with deionized water as the magnetic particles for the magnetic functional fluids. After this process, 0.075 g agar used as

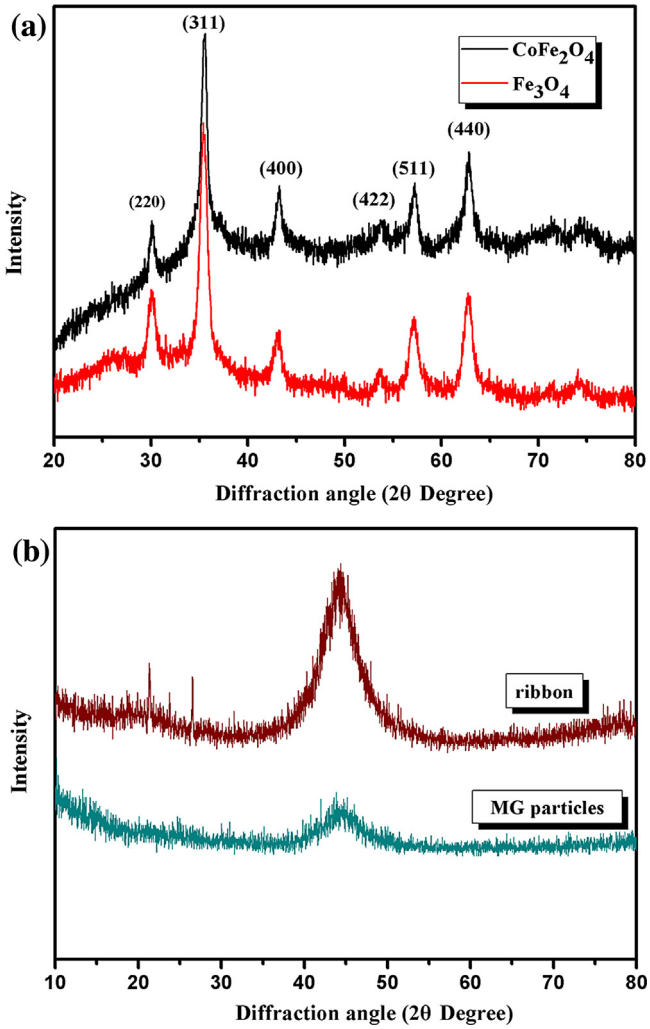

Fig. 2. The XRD patterns of Fe_3O_4 nanoparticles and $CoFe_2O_4$ nanoparticles (a), and $Fe_{73.5}Nb_3Cu_1Si_{13.5}B_9$ ribbons and particles (b).

the first surfactant was put into the mixture solution at a constant temperature of 55 °C. The mixture solution was kept at this temperature with stirring for 1 h. The resulting amorphous particles were isolated by magnet, washed several times with deionized water,

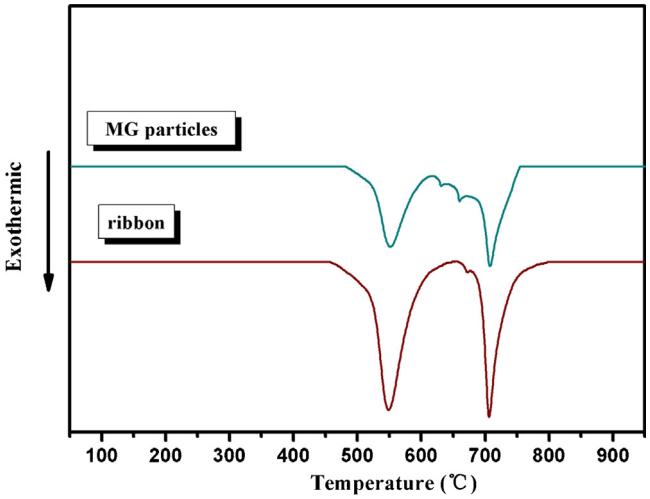

Fig. 3. DSC curves of $Fe_{73.5}Nb_3Cu_1Si_{13.5}B_9$ metallic glass ribbons and particles after being milled with a heating rate of 20 °C/min.

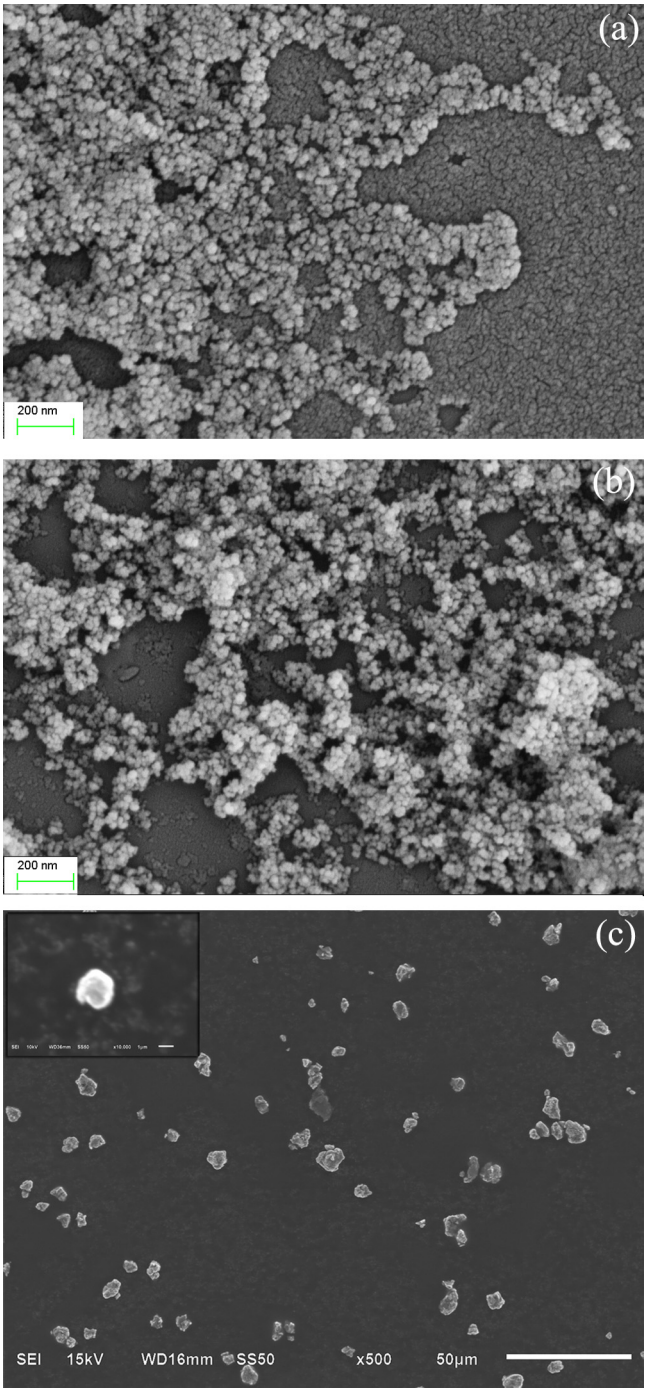

Fig. 4. SEM images of Fe_3O_4 nanoparticles, $CoFe_2O_4$ nanoparticles and $Fe_{73.5}Nb_3Cu_1Si_{13.5}B_9$ particles.

and transferred to a beaker. For further modifying the particles, the dilute hydrochloric acid was used to adjust the pH to 4–5. Then a certain amount of polyethylene glycol (0.05 g PEG-4000) was added to coat on the surface of the $Fe_{73.5}Nb_3Cu_1Si_{13.5}B_9$ amorphous particles as the second surfactant with stirring for 1 h at a constant temperature of 60 °C. Finally, after cooled to room temperature, a $Fe_{73.5}Nb_3Cu_1Si_{13.5}B_9$ MR fluid was obtained. Fig. 1 displays the schematic of preparation processing of $Fe_{73.5}Nb_3Cu_1Si_{13.5}B_9$ MR fluid, Fe_3O_4 FF and $CoFe_2O_4$ FF.

The structures of $Fe_{73.5}Nb_3Cu_1Si_{13.5}B_9$ amorphous particles, Fe_3O_4 nanoparticles and $CoFe_2O_4$ nanoparticles were characterized by X-ray diffraction (XRD) measurements carried out with

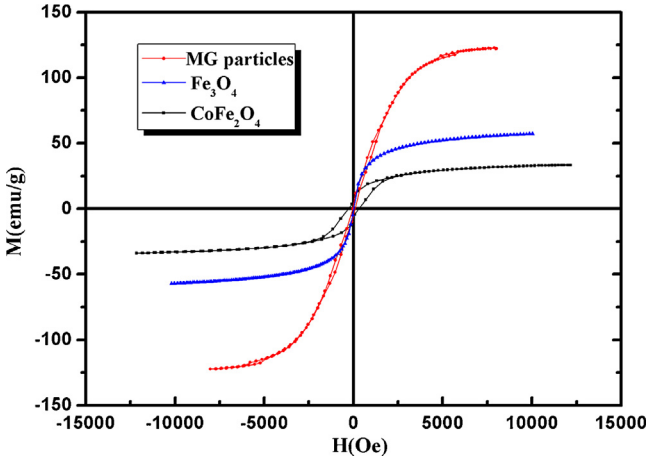

Fig. 5. Hysteresis curves of Fe_3O_4 nanoparticles, $CoFe_2O_4$ nanoparticles and $Fe_{73.5}Nb_3Cu_1Si_{13.5}B_9$ MG particles.

D/max-rB, using Cu Kα radiation. The characteristic of particles morphology was investigated by scanning electron microscopy (SEM). The magnetic properties of the particles and magnetic functional fluids were measured by a vibrating sample magnetometer (VSM) at room temperature. The hyperthermia effects of the $Fe_{73.5}Nb_3Cu_1Si_{13.5}B_9$ MR fluid, Fe_3O_4 FF and $CoFe_2O_4$ FF were investigated by a self-made device.

3. Results and discussion

Fig. 2 shows the X-ray diffraction patterns of Fe_3O_4 nanoparticles, $CoFe_2O_4$ nanoparticles and $Fe_{73.5}Nb_3Cu_1Si_{13.5}B_9$ particles. It indicates a series of characteristic peaks for (2 2 0), (3 1 1), (4 0 0), (4 2 2), (5 1 1) and (4 4 0) planes of Fe_3O_4 and $CoFe_2O_4$ as shown in Fig. 2(a). No obvious impurity peaks can be observed. The experimental data demonstrate the samples can be indexed to the cubic spinel structures. The average of crystallize size D is calculated using the Sherrer equation: $D = K\lambda/(\beta\cos\theta)$. The crystallite sizes of Fe_3O_4 and $CoFe_2O_4$ nanoparticles are found to be 12.9 nm and 13.4 nm, respectively. As can be seen in Fig. 2(b), both the $Fe_{73.5}Nb_3Cu_1Si_{13.5}B_9$ metallic glass ribbons and particles exhibit broad peaks around $2\theta = 45^\circ$, which are characteristics of amorphous structures. The broad peak of the particles is much weaker than that of the ribbons, which illustrates that the amorphous characteristic is weakened after being milled.

The differential scanning calorimeters (DSC) curves of the $Fe_{73.5}Nb_3Cu_1Si_{13.5}B_9$ metallic glass ribbons and particles obtained at heating rate of 20 °C/min are shown in Fig. 3. Two exothermic peaks during heating indicate two stages crystallization of the ribbons and particles, which reveals that the particles remain amorphous after being milled for 48 h. The results correspond well with the XRD data mentioned above.

Fig. 4(a)–(c) shows the morphologies of the Fe_3O_4 nanoparticles, $CoFe_2O_4$ nanoparticles and $Fe_{73.5}Nb_3Cu_1Si_{13.5}B_9$ particles, respectively. Fig. 4(a) and (b) illustrates that Fe_3O_4 nanoparticles and $CoFe_2O_4$ nanoparticles display a high degree of size homogeneity with typical size in the 10–15 nm. Observation in Fig. 4(c) reveals that the $Fe_{73.5}Nb_3Cu_1Si_{13.5}B_9$ particles after being milled appear to near-spheres with different sizes. The particle sizes could reach 8 μm or even smaller.

The magnetic properties of Fe_3O_4 nanoparticles, $CoFe_2O_4$ nanoparticles and $Fe_{73.5}Nb_3Cu_1Si_{13.5}B_9$ particles have been characterized by VSM at room temperature. The magnetic hysteresis cures are shown in Fig. 5. The results show that the saturation magnetization (Ms) of the Fe_3O_4 nanoparticles is about 58 emu/g.

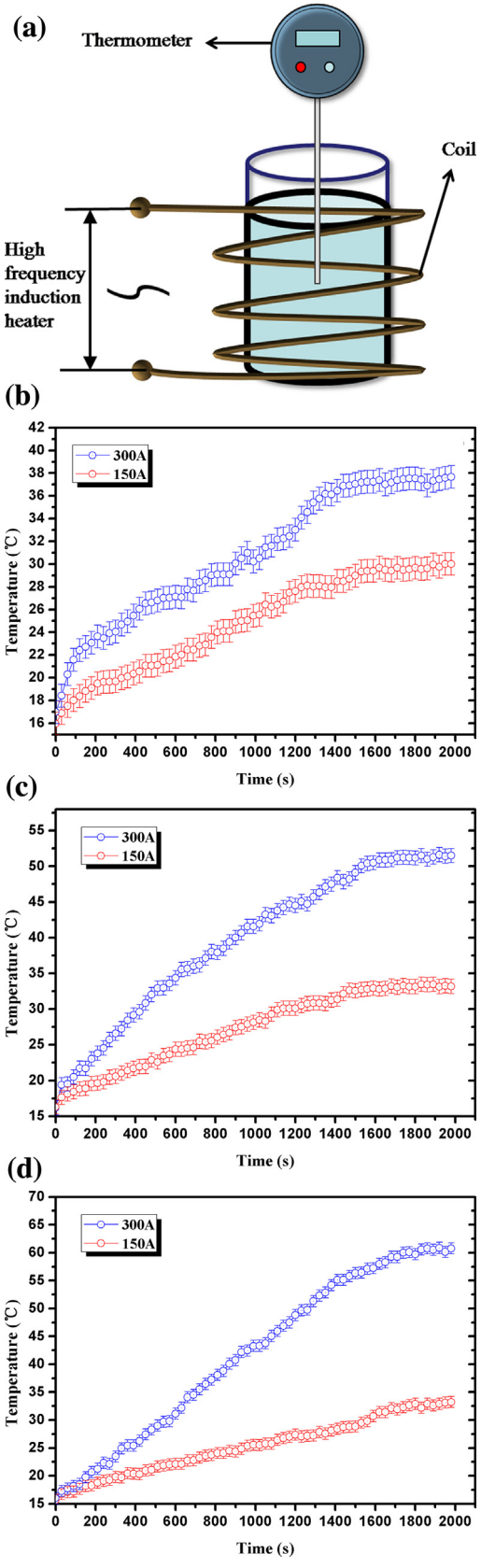

Fig. 6. (a) The schematic diagram of experimental setup for the magnetic heating experiment, (b) the heating curves of the $CoFe_2O_4$ FF, (c) the heating curves of the Fe_3O_4 FF, (d) the heating curves of the $Fe_{73.5}Nb_3Cu_1Si_{13.5}B_9$ MR fluid.

No remanence and coercivity are observed for the particles on the hysteresis cure, confirming the superparamagnetism of the particles. The Ms of the $CoFe_2O_4$ nanoparticles is about 34 emu/g with relative higher coercivity and remanence. While the Ms of $Fe_{73.5}Nb_3Cu_1Si_{13.5}B_9$ particles is about 125 emu/g, which is approximately 75% and 50% larger than that of $CoFe_2O_4$ nanoparticles and Fe_3O_4 nanoparticles, respectively. Moreover, the results show the $Fe_{73.5}Nb_3Cu_1Si_{13.5}B_9$ particles exhibit low coercivity and remanence.

Magnetic fluid hyperthermia induced by heating effects in an AC-magnetic field of the magnetic nanoparticles has attracted much attention because of its safe treatment with little physical or mental strain to the patient [23]. Here, we investigated the hyperthermia effects of $Fe_{73.5}Nb_3Cu_1Si_{13.5}B_9$ MR fluid, Fe_3O_4 FF and $CoFe_2O_4$ FF. The schematic diagram of experimental setup of the magnetic heating experiment is shown in Fig. 6(a). A thermometer was used to record the temperature. The accuracy of the thermometer is 0.1 °C in temperature and the temperature measurement error is within 1 °C. The tests were conducted under normal room temperature. The work frequency of the high-frequency induction heater was 90 kHz, which was in the range for biomedical applications (50–100 kHz) [24]. The heating experiments were performed under different output currents ranging from 150 to 300 A. 50 ml $Fe_{73.5}Nb_3Cu_1Si_{13.5}B_9$ MR fluid, 50 ml Fe_3O_4 FF and 50 ml $CoFe_2O_4$ FF with 5% mass fraction were investigated.

The experimental results are shown in Fig. 6(b)–(d). It can be seen that when different alternating electrical currents were output, the temperature of all the $Fe_{73.5}Nb_3Cu_1Si_{13.5}B_9$ MR fluid, Fe_3O_4 FF and $CoFe_2O_4$ FF increased obviously as time goes on. The increase rate of temperature accelerated with the increase of electrical current. When the current was 150 A, the temperature rose to 30.0 °C for $CoFe_2O_4$ FF, 33.1 °C for Fe_3O_4 FF, and 33.3 °C for $Fe_{73.5}Nb_3Cu_1Si_{13.5}B_9$ MR fluid in 1500 s. However, when the current was 300 A, the final stable temperature could reach to 37.6 °C, 51.4 °C and 60.7 °C for the $CoFe_2O_4$ FF, Fe_3O_4 FF and $Fe_{73.5}Nb_3Cu_1Si_{13.5}B_9$ MR fluid, respectively. The efficiency of hyperthermia effect of $Fe_{73.5}Nb_3Cu_1Si_{13.5}B_9$ MR fluid is about 38% and 15% higher than that of $CoFe_2O_4$ FF and Fe_3O_4 FF, respectively. The experimental results indicated that the intensity of alternating magnetic field induced by alternating electrical currents had effects on the hyperthermia effect of the three magnetic functional fluids. The heating effect could be controlled effectively by adjusting the value of the output current. Moreover, it could be concluded that the $Fe_{73.5}Nb_3Cu_1Si_{13.5}B_9$ MR fluid has more significant heating effect than that of $CoFe_2O_4$ FF and Fe_3O_4 FF in an alternating magnetic field, which indicates that the $Fe_{73.5}Nb_3Cu_1Si_{13.5}B_9$ MR fluid has potential on hyperthermia therapy of tumor.

4. Conclusions

Three kinds of magnetic functional fluids, $Fe_{73.5}Nb_3Cu_1Si_{13.5}B_9$ MR fluid, $CoFe_2O_4$ FF and Fe_3O_4 FF, have been successfully prepared. The $Fe_{73.5}Nb_3Cu_1Si_{13.5}B_9$ particles are still amorphous with typical size of about 8 μm after being milled for 48 h. The Ms of metallic glass particles is approximately 75% and 50% larger than that of $CoFe_2O_4$ nanoparticles and Fe_3O_4 nanoparticles, respectively. The hyperthermia experimental results indicate that the $Fe_{73.5}Nb_3Cu_1Si_{13.5}B_9$ MR fluid exhibits more significant heating effect than that of $CoFe_2O_4$ FF and Fe_3O_4 FF in an alternating magnetic field. Considering the hyperthermia effect, the $Fe_{73.5}Nb_3Cu_1Si_{13.5}B_9$ MR fluid had potential on hyperthermia therapy of tumor in biomedical applications.

Acknowledgments

The authors are grateful for the financial supports from the National Natural Science Foundation of China (Grant Nos. 51371107 and 51402170), Postdoctoral Science Foundation of China (Grant No. 2014M551900) and Scientific and Technological Project of Shandong Province (Grant No. 2013GGX10217).

References

[1] M.T. López-López, A. Gómez-Ramírez, L. Rodríguez-Arco, et al., Langmuir 28 (15) (2012) 6232.
[2] J. Rodríguez-López, H.C. Shum, L. Elvira, et al., J. Magn. Magn. Mater. 326 (2013) 220.
[3] S. Odenbach, Colloids Surf. A: Physicochem. Eng. Asp. 217 (1) (2003) 171.
[4] C.C. Yang, X.F. Bian, J.Y. Qin, et al., J. Mol. Liq. 196 (2014) 357.
[5] R.E. Rosensweig, Int. Sci. Technol. 7 (1966) 48.
[6] R.E. Rosensweig, Ferrohydrodynamics, Cambridge University Press, New York, 1985.
[7] S.S. Papell, Low viscosity magnetic fluid obtained by the colloidal suspension of magnetic particles, US Patent 3215572 (1965).
[8] J. Rabinow, AIEE Trans. 67 (1948) 1308.
[9] G. Bossis, O. Volkova, S. Lacis, et al., Lecture Notes in Physics, vol. 594, 2002, pp. 201.
[10] B.J. Park, F.F. Fang, H.J. Choi, Soft Matter 6 (2010) 5246.
[11] J.D. Carlson, D.M. Catanzarite, K.A.S. Clair, Int. J. Mod. Phys. B 10 (1996) 2857.
[12] C.C. Yang, X.F. Bian, T.X. Guo, et al., Soft Mater. 12 (2014) 346.
[13] H. Shokrollahi, Mater. Sci. Eng. C 33 (5) (2013) 2476.
[14] M. Davudabadi Farahani, F. Shemirani, M. Gharehbaghi, Talanta 109 (2013) 121.
[15] B. Andò, S. Baglio, A. Beninato, Procedia Eng. 25 (2011) 559.
[16] R.X. Zheng, H. Yang, T. Liu, et al., Mater. Des. 53 (2014) 512.
[17] C.C. Yang, X.F. Bian, J.F. Yang, Funct. Mater. Lett. 7 (3) (2014) 1450028.
[18] G.I. Mamniashvili, S.V. Mikeladze, T.O. Gegechkori, et al., World J. Condens. Matter Phys. 4 (2014) 6.
[19] E. Auzans, D. Zins, E. Blums, et al., J. Mater. Sci. 34 (1999) 1253.
[20] R.N. Singh, J. Mater. Eng. Perform. 15 (2006) 422.
[21] Y.H. Tian, G.H. Su, J. Wang, et al., Progr. Nucl. Energy 68 (2013) 177.
[22] Y. Zheng, Z.Z. He, J. Yang, et al., Sci. Rep. 4 (2014) 4588.
[23] A. Inukai, N. Sakamoto, H. Aono, et al., J. Magn. Magn. Mater. 323 (7) (2011) 965.
[24] T. Minamimura, H. Sato, S. Kasaoka, et al., Int. J. Oncol. 16 (2000) 1153.